



Comparison of Neuronal Death, Blood–Brain Barrier Leakage and Inflammatory Cytokine Expression in the Hippocampal CA1 Region Following Mild and Severe Transient Forebrain Ischemia in Gerbils

Choong-Hyun Lee¹ · Ji Hyeon Ahn^{2,3} · Tae-Kyeong Lee⁴ · Hyejin Sim³ · Jae-Chul Lee³ · Joon Ha Park⁵ · Myoung Cheol Shin⁶ · Jun Hwi Cho⁶ · Dae Won Kim⁷ · Moo-Ho Won³ · Soo Young Choi⁴

Received: 22 February 2021 / Revised: 13 May 2021 / Accepted: 24 May 2021 / Published online: 29 May 2021
© The Author(s), under exclusive licence to Springer Science+Business Media, LLC, part of Springer Nature 2021

Abstract

Transient ischemia in the brain causes blood–brain barrier (BBB) breakdown and dysfunction, which is related to ischemia-induced neuronal damage. Leakage of plasma proteins following transient ischemia is one of the indicators that is used to determine the extent of BBB dysfunction. In this study, neuronal damage/death, leakage of albumin and IgG, microgliosis, and inflammatory cytokine expression were examined in the hippocampal CA1 region, which is vulnerable to transient ischemia, following 5-min (mild) and 15-min (severe) ischemia in gerbils induced by transient common carotid arteries occlusion (tCCAO). tCCAO-induced neuronal damage/death occurred earlier and was more severe after 15-min tCCAO vs. after 5-min tCCAO. Significant albumin and IgG leakage (albumin and IgG immunoreactivity) took 1 or 2 days to begin, and immunoreactivity was markedly increased 5 days after 5-min tCCAO. While, albumin and IgG leakage began to increase 6 h after 15-min tCCAO and remained significantly higher over time than that seen in 5-min tCCAO. IgG immunoreactivity was observed in degenerating neurons and activated microglia after tCCAO, and microglia were activated to a greater extent after 15-min tCCAO than 5-min tCCAO. In addition, following 15-min tCCAO, pro-inflammatory cytokines [tumor necrosis factor alpha (TNF- α) and interleukin 1 beta (IL-1 β)] immunoreactivity was significantly higher than that seen following 5-min tCCAO, whereas immunoreactivity of anti-inflammatory cytokines (IL-4 and IL-13) was lower in 15-min than 5-min tCCAO. These results indicate that duration of tCCAO differentially affects the timing and degree of neuronal damage or loss, albumin and IgG leakage and inflammatory cytokine expression in brain tissue. In addition, more severe BBB leakage is closely related to acceleration of neuronal damage through increased microglial activation and pro-inflammatory cytokine expression in the ischemic hippocampal CA1 region.

Keywords BBB disruption and leakage · Neuronal death · Ischemic duration · Ischemia-reperfusion injury · Microglia · Neuroinflammation

Choong-Hyun Lee and Ji Hyeon Ahn are co-first authors and contributed equally to this article.

✉ Moo-Ho Won
mhwon@kangwon.ac.kr

✉ Soo Young Choi
sychoi@hallym.ac.kr

Extended author information available on the last page of the article

Introduction

Transient ischemia in brains is known to be induced by temporary and marked reduction of cerebral blood flow, and causes selective neuronal damage/death (loss) in vulnerable brain regions [1, 2]. The hippocampus is composed of CA1-3 regions, and it is known that the pyramidal neurons of the CA1 region is most vulnerable [3, 4] and the pyramidal neurons of the CA3 region is relatively resistant to transient ischemia [5–7]. Death (loss) of pyramidal neurons in the CA1 region occurs at 4–5 days after 5-min transient ischemia; this phenomenon is called “delayed neuronal death (DND)” [3,

8]; although interneurons in the CA1 region are resistant to ischemia [9, 10]. Researchers studying the mechanisms of DND have suggested glutamate-mediated excitotoxicity, oxidative stress and neuroinflammatory process [11–14].

BBB dysfunction and endothelial damage, which are considered common pathological features, are seen in various neurologic conditions such as ischemic stroke [15], epilepsy [16], and multiple sclerosis [17]. Cerebral ischemia-induced increases in oxidative stress and neuroinflammation are known to promote BBB breakdown after cerebral ischemia, and the disruption and increased permeability of the BBB occurs rapidly and persists for days after onset of cerebral ischemia [18–20]. In addition, it is generally accepted that BBB dysfunction is one of the important mechanisms of ischemia-induced neuronal damage and that the preservation of BBB integrity may have a neuroprotective effect cerebral ischemic damage [21–26].

Several methods, such as measurement of exogenous dyes or blood proteins, to assess changes in BBB permeability following cerebral ischemia have been introduced [18]. Among them, extravasation and accumulation of endogenous serum albumin and IgG following cerebral ischemia is one of the most widely used indicators of BBB disruption [22, 27–29]. Previous studies have investigated the distribution of serum proteins to elucidate the relationship between leaked serum proteins and neuronal cell death in the brain over time after transient ischemia. Notably, gliosis has been identified in areas containing serum protein exudate after ischemia [27, 30, 31].

Recently, we reported that neuronal damage and glial activation in the hippocampus were distinct entities following various durations of transient ischemia [32, 33]. However, while BBB dysfunction has been suggested as one of the causes of ischemic neuronal death, especially in the hippocampus, which is a brain structure that is more vulnerable to transient ischemia compared to the cortex [34], striatum [35], and septum [36], the relationship between neuronal damage according to the ischemic duration, BBB dysfunction, and inflammatory factors has not yet been fully elucidated. Therefore, the aim of this study was to examine differences in neuronal damage, leakage of albumin and IgG, microgliosis, and inflammatory cytokines in the gerbil hippocampus following 5-min (mild) and 15-min (severe) ischemia through transient common carotid arteries occlusion (tCCAo).

Materials and Methods

Experimental Animals, Protocol and Groups

Male Mongolian gerbils at six months of age (body weight, 64–76 g) were obtained from the Experimental Animal

Center of Kangwon National University (Chuncheon, South Korea). They were cared under constant temperature (23 °C) and humidity (55%) with a 12-h light/dark cycle. The handling and caring of the gerbils conformed to the guidelines in the “Current international laws and policies” included in the “NIH Guide for the Care and Use of Laboratory Animals” published by The National Academies Press (8th Ed., 2011). Experimental protocol including animal care and handling was approved (approval no. KW-2000113-1) on 13th, January, 2020 by Institutional Animal Care and Use Committee (IACUC) of Kangwon National University (South Korea).

Gerbils (total $n = 140$) were assigned to four groups: (1) 5-min sham tCCAo operated (5-min sham) group (subtotal $n = 35$); (2) 5-min tCCAo operated (5-min tCCAo) group (subtotal $n = 35$); (3) 15-min sham tCCAo operated (15-min sham) group (subtotal $n = 35$); (4) 15-min tCCAo operated (15-min tCCAo) group (subtotal $n = 35$).

Induction of tCCAo

As previously described in our published papers [32, 37, 38], surgical procedure of tCCAo was performed as follows. Briefly, the gerbils were anesthetized with mixture of 2.5% isoflurane (Baxter, Deerfield, IL, USA) in 33% oxygen and 67% nitrous oxide. Under the anesthesia, common carotid arteries located at both sides in the neck were isolated from the carotid sheath and ligated for 5 and 15-min for mild and severe tCCAo, respectively. During tCCAo induction, body temperature was checked with a rectal temperature probe and controlled at normothermic condition (37 ± 0.5 °C) by using a thermometric blanket. The gerbils of the sham group received the same surgical operation without occlusion of the carotid arteries.

Preparation of Brain Sections

Sections containing the hippocampus were prepared as previously described studies [32, 37, 38]. In brief, the gerbils in each group ($n = 7$ at each point in time) were anesthetized with 70 mg/kg pentobarbital sodium at designated times (6 h, 12 h, 1 day, 2 days and 5 days after tCCAo). Under anesthesia, the brains of the gerbils were washed by perfusion with saline and fixed by perfused with 4% paraformaldehyde solution (in 0.1 M phosphate-buffer (PB), pH 7.4). The brains were removed and more fixed in the fixative for 6 h. Thereafter, the brain tissues were infiltrated with 30% sucrose solution to avoid tissue damage from freeze. These brain tissues were sectioned into 30- μ m thickness of frontal sections in a cryostat, and then they were stored in well plates containing PBS (pH 7.4) until histological staining.

Histofluorescence with Fluoro-Jade B (FJB)

Histofluorescence with FJB (a fluorescent marker of cellular degeneration or death) was carried out to examine damage/death of cells or neurons in gerbil hippocampus after TI. In short, as described in our published papers [32, 37], the prepared brain sections were immersed in solution of 0.06% potassium permanganate and stained with solution of 0.0004% F-J B (Histochem, Jefferson, AR, USA).

The count of FJB positive cells was counted in a $250 \times 250 \mu\text{m}^2$ at the middle of the CA1 region according to our published method [32, 37]. Eight sections with 90- μm interval were selected in reference to anatomical landmarks of the gerbil brain atlas [39]. The cells were observed with a fluorescence microscope from Carl Zeiss with blue excitation fluorescence filter between 450–490 nm (Göttingen, Germany). Images of the cells, which underwent degeneration with bright fluoresce in comparison to the background [40], were captured and counted with Image J 1.59 software (United States National Institute of Health).

Immunohistochemistry

The antibodies used in this study were Neuronal nuclear antigen (NeuN) for detection of intact neurons, albumin and IgG for detection for BBB leakage, TNF- α and IL-1 β for pro-inflammatory cytokines, IL-4 and IL-13 for anti-inflammatory cytokines, and Iba-1 for detection of microglial cells. The dilution and source of each antibody was as follows: mouse anti-NeuN (diluted 1:1,000, Millipore, Billerica, MA, USA), mouse anti-albumin (diluted 1:100, Abcam, Cambridge, MA), rabbit anti-gerbil IgG antibody (diluted 1:1,000, Bioss antibodies, Atlanta, GA, USA), rabbit anti-TNF- α (diluted 1:1000, Abcam, Cambridge, MA, USA), rabbit anti-IL-1 β (diluted 1:200, Santa Cruz Biotechnology, Santa Cruz, CA, USA), rabbit anti-IL-4 (diluted 1:200, Santa Cruz Biotechnology, CA), rabbit anti-IL-13 (diluted 1:200, Santa Cruz Biotechnology, CA) and rabbit anti-Iba-1 (diluted 1:800, Wako Chemicals, Japan). Immunohistochemical staining was conducted according to our published method [32, 37, 38]. In brief, the sections were incubated in each solution of antibody for 12 h at 4 °C. Thereafter the sections were incubated in biotinylated horse anti-mouse (diluted 1:250, Vector, Burlingame, CA, USA) and goat anti-rabbit (diluted 1:250, Vector, Burlingame, CA, USA), followed by streptavidin peroxidase complex (diluted 1:250, Vector, Burlingame, CA). Finally, to change the end product into brown, the sections were reacted in 3,3'-diaminobenzidine tetrahydrochloride (DAB) solution.

The count of NeuN immunoreactive neurons was performed according to our published methods [3]. Briefly, NeuN immunoreactive neurons were counted in a $250 \times 250 \mu\text{m}^2$ at the center of the CA1 region using Image

J 1.59 software (United States National Institute of Health). Five sections were selected with 120 μm interval in reference to anatomical landmarks of the gerbil brain atlas [39], and cell counts were carried out by averaging the counts from each animal. Quantitative analyses of albumin, IgG, TNF- α , IL-1 β , IL-4, IL-13 immunoreactivities were evaluated as relative optical density (ROD) as %, as described in our published papers [32, 37, 38]. In short, digital images of the albumin, IgG, TNF- α , IL-1 β , IL-4, and IL-13 immunoreactive structures were captured in all layers of the CA1 region with the light microscope (BX53). The background was taken from the areas adjacent to the measured area. ROD was calibrated by using Adobe Photoshop version 8.0 and Image J 1.59 software (United States National Institute of Health) according to method by Sugawara et al. [41].

Double Immunofluorescence Staining

Double immunofluorescence staining was carried out to identify cell types containing IgG immunoreactivity. Primary antibodies were rabbit anti-gerbil IgG (diluted 1:500, Gene Tex, Inc., Irvine, CA, USA)/goat anti-Iba1 (1:100, abcam, Cambridge, MA, USA) to detect IgG localization in microglia and IgG/mouse anti-NeuN (diluted 1:1000, Millipore, Billerica, MA, USA) to detect IgG localization in neurons. In brief, as described in our published papers [37, 38, 42]. The sections were incubated in the mixture of the antisera, followed by reacting in mixture of goat anti-rabbit IgG conjugated to Alexa Fluor488 (diluted 1:500, Invitrogen, Waltham, MA, USA) and donkey anti-goat IgG conjugated to Alexa Fluor546 (diluted 1:500, Invitrogen, USA) or goat anti-mouse IgG conjugated to Alexa Fluor 546 (diluted 1:500, Invitrogen, USA).

The double immunoreaction was observed with a fluorescence microscope from Carl Zeiss (Göttingen, Germany).

Statistical Analysis

Data shown in this study represent the mean \pm standard deviation (SD) among experimental groups. The data were statistically analyzed by using SPSS 18.0 (SPSS, Chicago, IL, USA). Analysis of variance (ANOVA) with a post hoc Bonferroni's multiple comparison test was done to determine differences among groups. $P < 0.05$ was used for statistical significance.

Results

Neuronal Death After tCCAO

NeuN antibody was used for detection of neurons in the hippocampus. NeuN immunoreactivity was changed after

neuronal damage. In both the 5-min sham tCCAo operated (5-min sham) group and 15-min sham tCCAo operated (15-min sham) groups, strong NeuN immunoreactivity was shown in pyramidal neurons located at the stratum pyramidale in the CA1 region (Fig. 1A, B, a, and b). At 2 days after tCCAo, the distribution pattern and numbers of NeuN⁺ pyramidal neurons were not changed after 5-min tCCAo (Fig. 1C, D and G); however, in the 15-min tCCAo group, the numbers of NeuN-immunoreactive(+) pyramidal neurons were significantly reduced (48.0% of the sham group) (Fig. 1c, d and G). Five days after tCCAo, a few NeuN⁺ pyramidal neurons (15.7% and 10.1% of the sham groups, respectively) were found in both 5-min tCCAo and 15-min tCCAo groups (Fig. 1E, F, e, f and G).

FJB is a fluorescent marker of cellular degeneration or death. In this study, histofluorescence with FJB was used to detect damaged or dead cells in gerbil hippocampus after tCCAo. In all sham groups, no FJB positive(+) cells were shown in the CA1 region (Fig. 2A, B, and G). Two days after 5-min and 15-min tCCAo, FJB⁺ cells were not found after 5-min tCCAo (Fig. 2C, G); however, many FJB⁺ cells were shown in the SP after 15-min tCCAo (Fig. 2D, G). At 5 days after tCCAo, many FJB⁺ cells were detected in the SP of the 5-min tCCAo group (Fig. 2E, G), and, at this point in time, the number of FJB⁺ cells in the 15-min tCCAo group was higher (110.1%) than that in the 5-min tCCAo group (Fig. 2F and G).

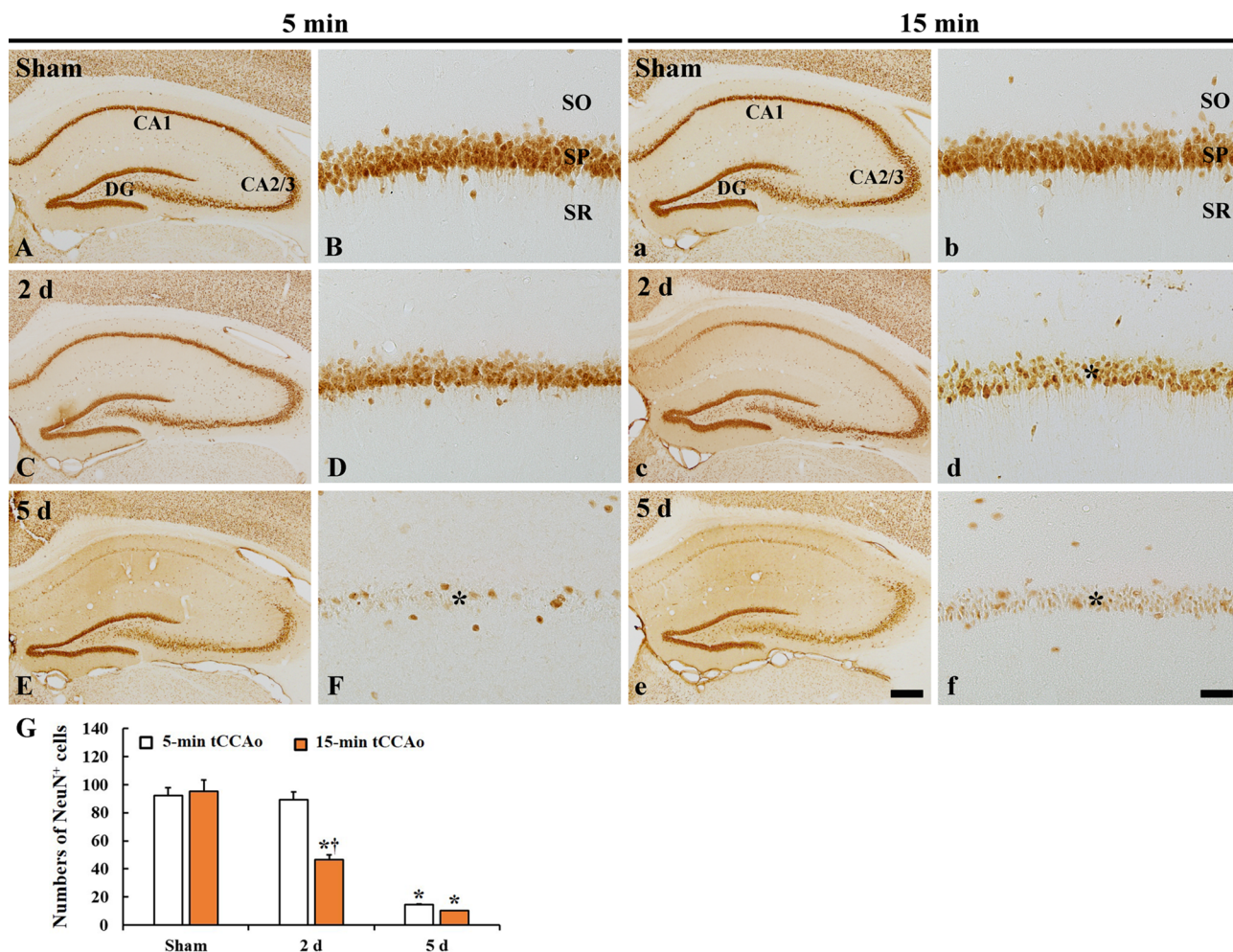
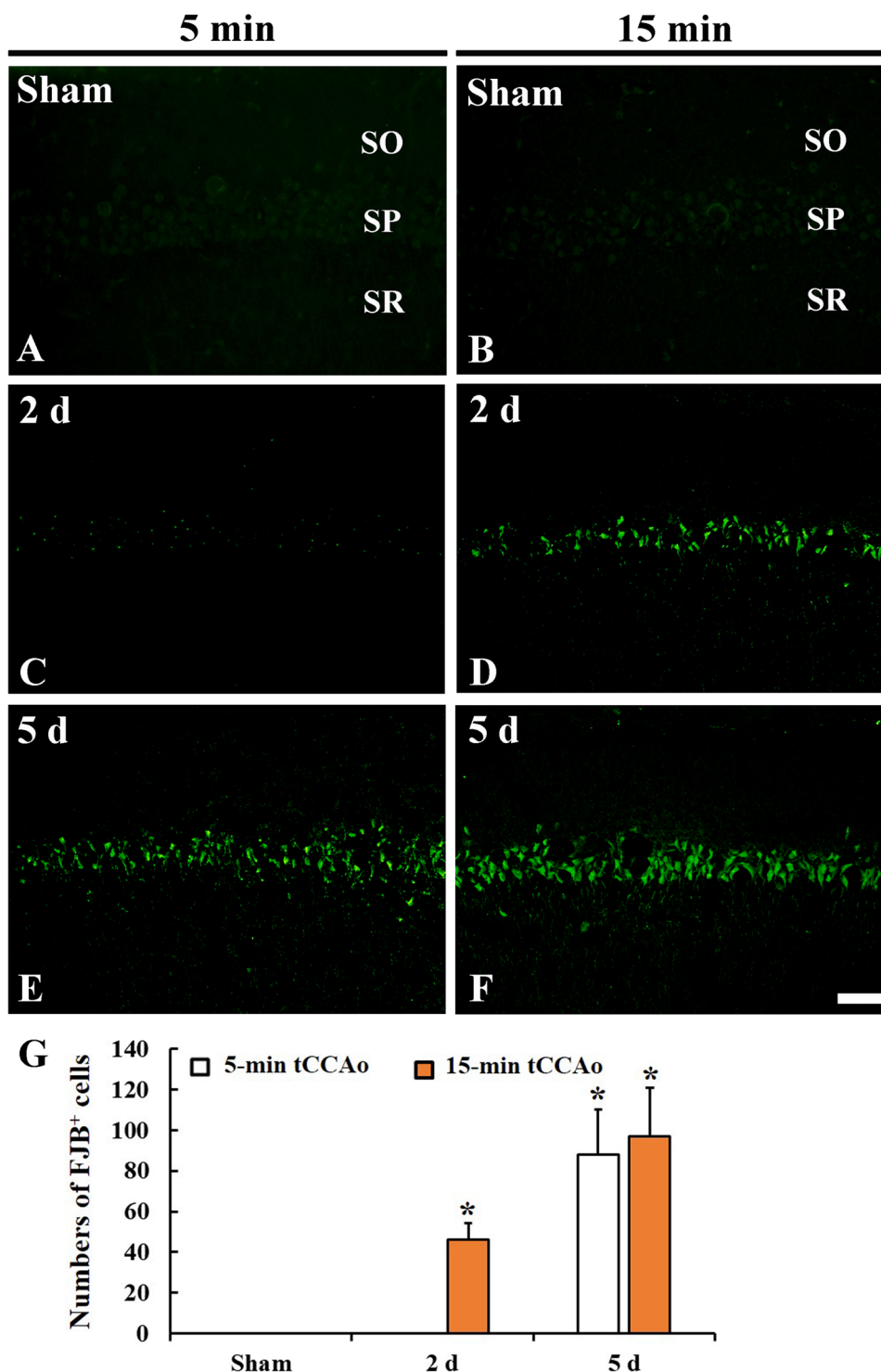


Fig. 1 Immunohistochemical staining for NeuN in the CA1 region at sham (A, B, a, b), 2 days (C, D, c, d) and 5 days (E, F, e, f) in the 5-min (A–F) and 15-min (a–f) tCCAo groups. NeuN⁺ pyramidal neurons are significantly decreased in number at 2 days after 15-min tCCAo, not 5-min tCCAo. Five days after tCCAo, a few NeuN⁺ pyramidal neurons are observed in both the 5-min tCCAo and 15-min

tCCAo groups. SO, stratum oriens; SP, stratum pyramidale; SR, stratum radiatum. Scale bar = 200 μm (A, C, E, a, c, e), 50 μm (B, D, F, b, d, f). **G** Numbers of NeuN⁺ neurons in the SP. The bars indicate the means ± SD (n = 7 at each time after tCCAo, *P < 0.05, significantly different from the sham groups, †P < 0.05, significantly different from the 5-min tCCAo group)

Fig. 2 FJB histofluorescence in the CA1 region at sham (A, B), 2 days (C, D) and 5 days (A, B, E and F) in the 5-min (A, C and E) and 15-min (B, D and F) tCCAo groups. FJB⁺ cells are found in the SP at 2 days after 15-min tCCAo, not 5-min tCCAo. Five days after tCCAo, numerous FJB⁺ cells are shown in the SP after 5-min and 15-min tCCAo. Scale bar = 50 μ m. **G** Numbers of FJB⁺ cells in the SP. The bars indicate the means \pm SD (n = 7 at each time after tCCAo, *P < 0.05, significantly different from the sham groups)



BBB Leakage After tCCAo

In the present study, albumin immunohistochemistry was conducted to examine BBB leakage following tCCAo induced BBB dysfunction in the hippocampal CA1 region. In all sham groups, albumin immunoreactivity was observed inside blood vessels in the CA1 region (Fig. 3a, a1). In the

5-min tCCAo group, no marked change in albumin immunoreactivity was found at 6 h and 12 h after tCCAo compared to that in the sham group (Fig. 3b, c and g). However, albumin immunoreactivity began to increase at 1 day (384.1% of the sham group) after tCCAo, and thereafter albumin immunoreactivity was gradually increased throughout the CA1 region, showing that, at 5 days after 5-min tCCAo,

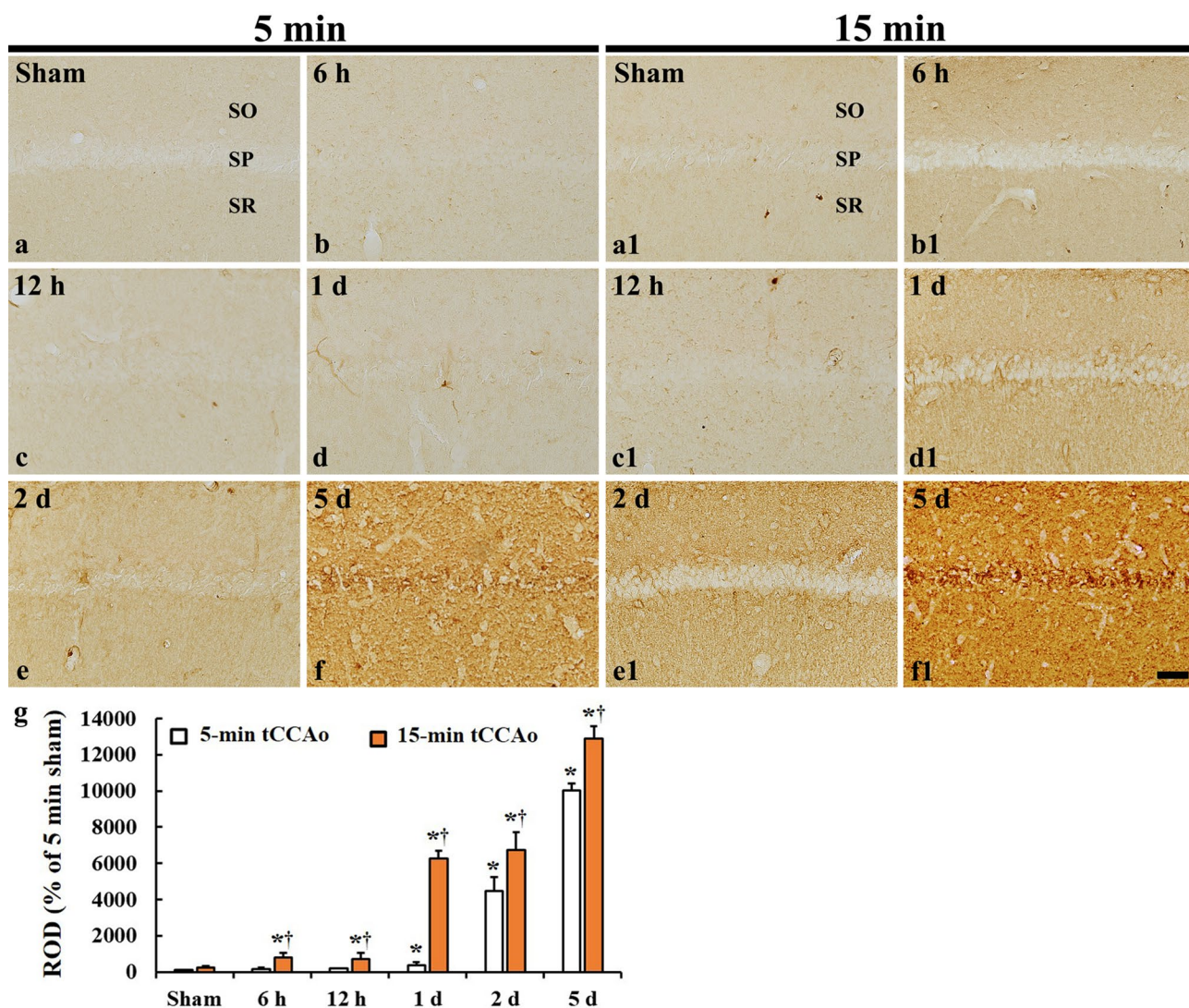


Fig. 3 Immunohistochemistry for albumin in the CA1 region at sham (a, a1), 6 h (b, b1), 12 h (c, c1), 1 day (d, d1), 2 days (e, e1), and 5 days (f, f1) in the 5-min (a–f) and 15-min (a1–f1) tCCAo groups. Albumin immunoreactivity is gradually increased in both groups, and the immunoreactivity at corresponding time after tCCAo is

much higher in the 15-min tCCAo group than that in the 5-min tCCAo group. Scale bar=50 μm. (g) ROD of albumin immunoreactive structures. The bars indicate the means±SD (n=7 at each time after tCCAo, *P<0.05, significantly different from the sham groups, †P<0.05, significantly different from the 5-min tCCAo group)

albumin immunoreactivity was 9925.2% of the sham group (Fig. 3d–g). In the 15-min tCCAo group, albumin immunoreactivity in the CA1 region was significantly increased from 6 h, showing that albumin immunoreactivity at 1 day, 2 days and 5 days was 6256.1%, 6732.8% and 12,902.4%, respectively, of that in the 5-min tCCAo group (Fig. 3b1–f1 and g). In particular, at 1 day after 15-min tCCAo, albumin immunoreactivity was highly observed around vessels (Fig. 3d1). In addition, very intense albumin immunoreactivity was shown in the SP at 5 days after 15-min tCCAo (Fig. 3f1).

In the present study, IgG immunohistochemistry was conducted to examine BBB leakage following tCCAo-induced BBB dysfunction in the hippocampal CA1

region. In both sham groups, IgG immunoreactivity was observed inside blood vessels and no IgG extravasation was not found in the CA1 region after 5-min and 15-min tCCAo (Fig. 4a, a1). In the 5-min tCCAo group, there was no significant change in IgG immunoreactivity at 6 h and 12 h after tCCAo compared with that in the sham group (Fig. 4b, c and g). However, one day after 5-min tCCAo, IgG immunoreactivity in the CA1 region was significantly increased and the immunoreactivity was gradually increased with time after tCCAo (Fig. 4d–f), showing that, at 5 days after tCCAo, IgG immunoreactivity was 4662.8% of the sham group (Fig. 4g). Interestingly, IgG immunoreactivity was newly observed in cellular

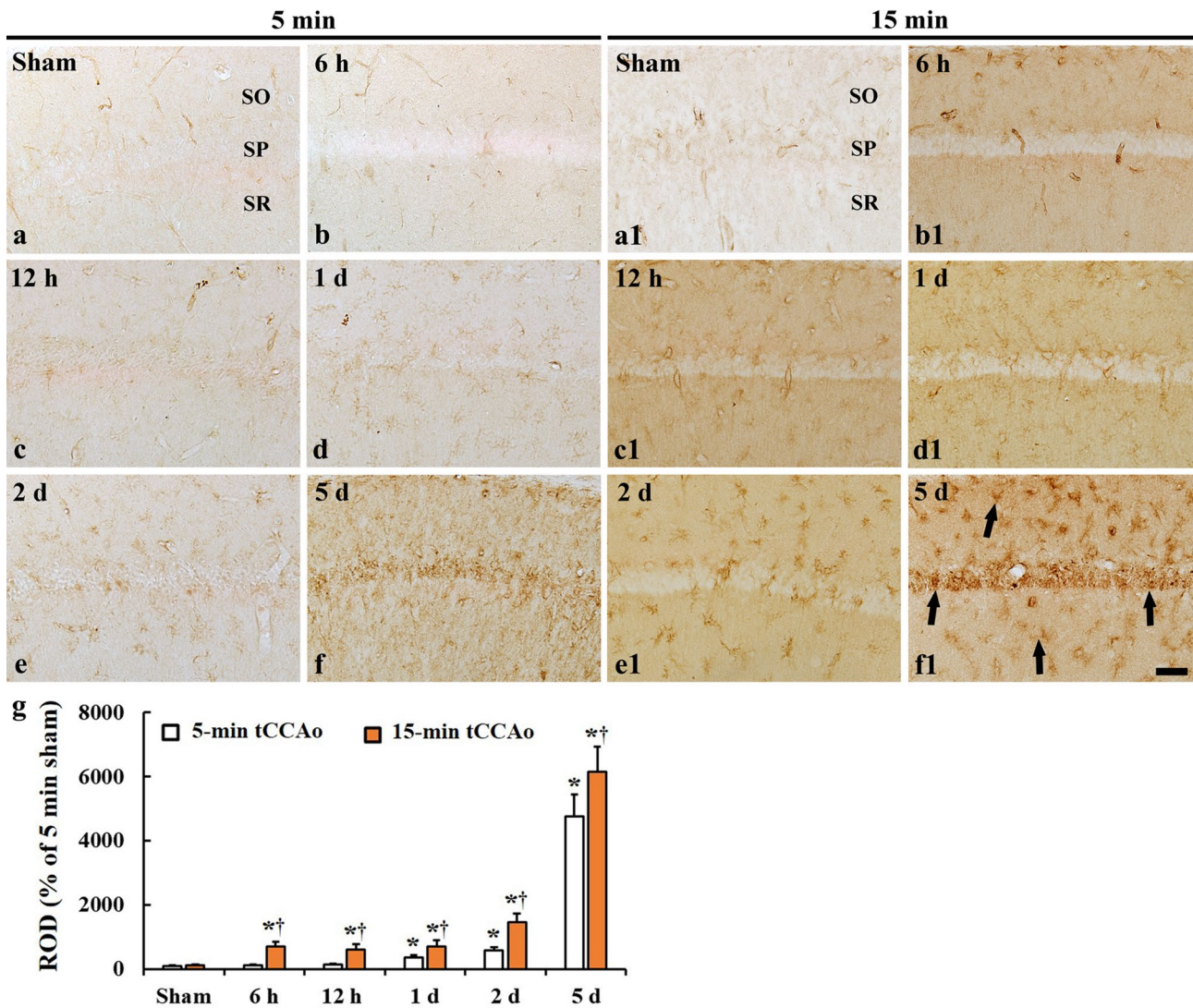


Fig. 4 Immunohistochemistry for IgG in the CA1 region at sham (**a**, **a1**), 6 h (**b**, **b1**), 12 h (**c**, **c1**), 1 day (**d**, **d1**), 2 days (**e**, **e1**), and 5 days (**f**, **f1**) in the 5-min (**a–f**) and 15-min (**a1–f1**) tCCAo groups. In all sham groups, IgG immunoreactivity is observed in blood vessels. IgG extravasation is found from 1 day after 5-min tCCAo and from 6 h after 15-min tCCAo. IgG immunoreactivity in the 15-min tCCAo group is much higher than that in the 5-min tCCAo group at

each corresponding time after tCCAo. Note that strong IgG immunoreactivity is shown in cellular components (arrows) at 5 days after 15-min tCCAo. Scale bar=50 μ m. (**g**) ROD of IgG immunoreactive structures. The bars indicate the means \pm SD ($n=7$ at each time after tCCAo, * $P<0.05$, significantly different from the sham groups, † $P<0.05$, significantly different from the 5-min tCCAo group)

components throughout the CA1 region from 1 day after tCCAo (Fig. 4d–f). In the 15-min tCCAo group, strong IgG immunoreactivity was found in neuropil and around blood vessels and in neuropil at 6 h after 15-min tCCAo (Fig. 4b1), and thereafter IgG immunoreactivity was gradually increased, showing that, at 5 days after tCCAo, very strong IgG immunoreactivity (6031.6% of the sham group) was shown (Fig. 4f1 and g). In addition, IgG immunoreactivity at 5 days after tCCAo, IgG immunoreactivity in the cellular components was stronger and clearer than that at 5 days after 5-min tCCAo (Fig. 4f1, g).

To identify cell types expressing IgG immunoreactivity, double immunofluorescence staining was performed for IgG/ionized calcium-binding adapter molecule 1 (Iba-1, a marker for microglia) and IgG/NeuN (a marker for neurons) in the CA1 region at 5 days after 15-min tCCAo. IgG immunoreactivity was shown in Iba-1-immunoreactive microglia throughout the CA1 region (Fig. 5A–C) and colocalized with NeuN-immunoreactive pyramidal neurons (Fig. 5D–F).

Microglial Activation After tCCAO

In this study, microglial cells were immunohistochemically stained using Iba-1 antibody to examine change in microgliosis. In both sham groups, Iba-1 immunoreactive microglia, as a resting form, had small cytoplasm and thin recesses, and they were distributed in all layers of the CA1 region (Fig. 6A, B). In the 5-min tCCAO group, the cytoplasm of Iba-1 immunoreactive microglia was hypertrophied, and their processes were thickened after tCCAO (Fig. 6C, E and GI), showing that the ROD of the Iba-1 immunoreactivity was significantly increased with time (153.7%, 219.4% and 502.6%, respectively, at 1 day, 2 days and 5 days after 5-min tCCAO compared with that in the sham group) (Fig. 6I). Interestingly, at 5 days after 5-min tCCAO, Iba-1 immunoreactive microglia were aggregated in the stratum pyramidale (Fig. 6E). In the 15-min tCCAO group, the activation of Iba-1 immunoreactive microglia after 15-min tCCAO was higher than that in the 5-min tCCAO group (Fig. 6D, F and H), showing that the ROD of the Iba-1 immunoreactivity was much higher than that in the 5-min tCCAO group (214.2% at 1 day, 456.7% at 2 days and 733.1% at 5 days after 15-min tCCAO compared with that in the sham group) (Fig. 6I).

Changes of Pro-Inflammatory and Anti-Inflammatory Cytokines After tCCAO

In this study, TNF- α and IL-1 β immunohistochemistry was conducted to examine the changes of pro-inflammatory cytokines following tCCAO in the hippocampal CA1 region.

In both sham groups, TNF- α immunoreactivity was shown in pyramidal cells (Fig. 7Aa, Aa1), showing that the immunoreactivity was not different between the 5-min sham and 15-min sham groups (Fig. 7C). In the 5-min tCCAO group, TNF- α immunoreactivity in the pyramidal cells was gradually and significantly increased from 6 h to 1 day after tCCAO (163.6% at 6 h, 248.1% at 12 h and 410.2% at 1 day compared with that in the 5-min sham group) (Fig. 7Ab, Ac and Ad and C), thereafter TNF- α immunoreactivity was decreased (365.2% at 2 days and 56.6% at 5 days compared with that in the 5-min sham group) (Fig. 7Ae, Af and C). In the 15-min tCCAO group, TNF- α immunoreactivity in the pyramidal neurons was also increased from 6 h after tCCAO to 1 day after tCCAO, showing that its ROD was significantly higher (224.8% at 6 h, 469.6% at 12 h and 515.4% at 1 day) than that in the 5-min sham group (Fig. 7Aa1, Ab1, Ac1 and C). Thereafter, TNF- α immunoreactivity was also gradually decreased, but its ROD was higher (217.3% at 2 days

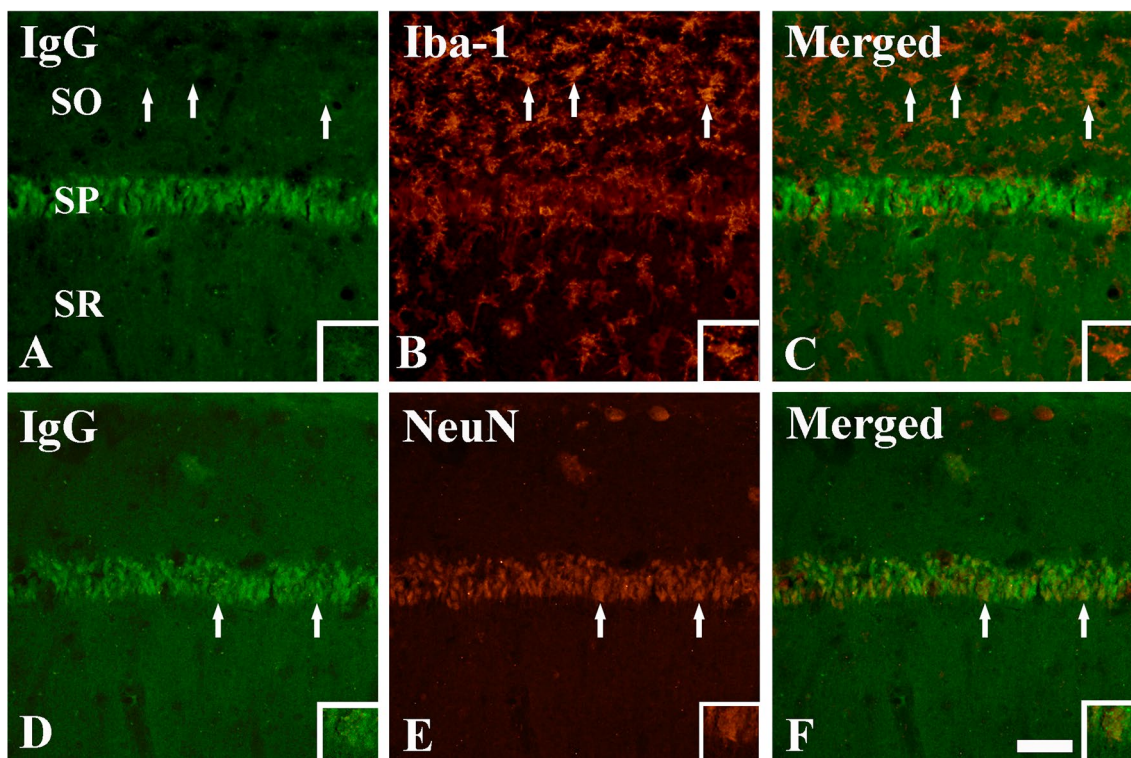


Fig. 5 Double immunofluorescence staining for IgG (green, **A** and **D**), Iba-1 (red, **B**) or NeuN (red, **E**), and merged images (**C**, **F**) in the CA1 region at 5 days after 15-min tCCAO. IgG immunoreactiv-

ity is localized in Iba-1-immunoreactive microglia (arrows in **C**) and NeuN-immunoreactive neurons (arrows in **F**). Scale bar = 50 μ m

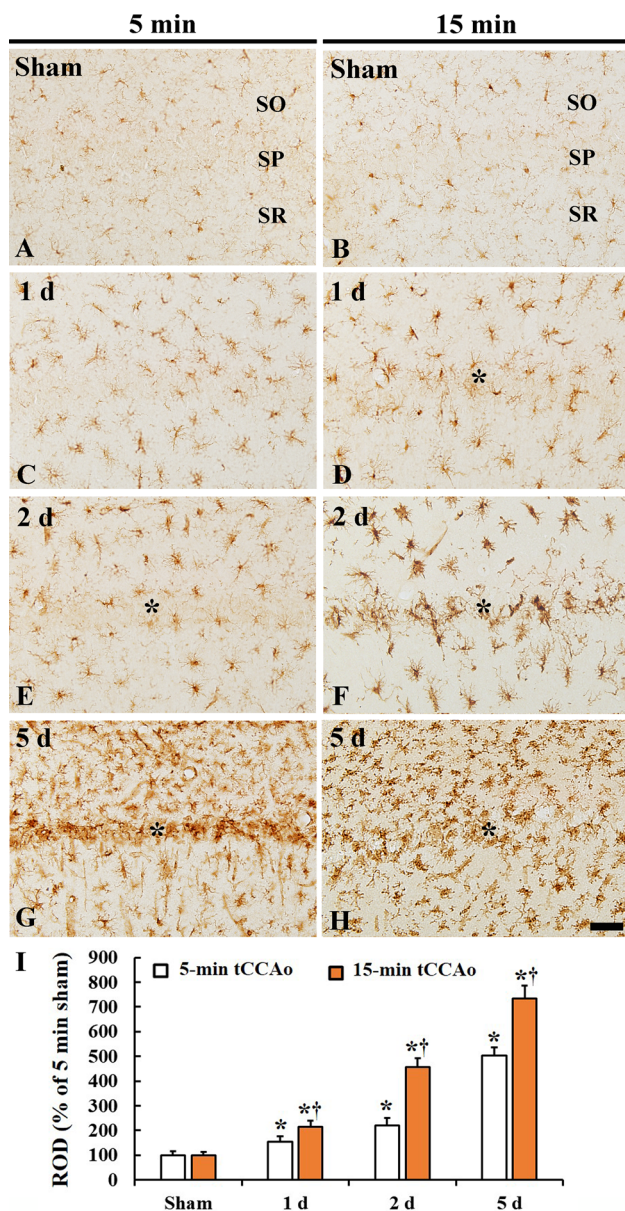


Fig. 6 Immunohistochemistry for Iba-1 in the CA1 region at sham (A, B) and 1 day (C, D), 2 days (E, F) and 5 days (G, H) in the 5-min (A, C, E and G) and 15-min (B, D, F and H) tCCAo groups. Iba-1 immunoreactive microglia are activated (hypertrophied cell body and thickened processes) after 5-min tCCAo and 15-min tCCAo, showing that the activation in the 15-min tCCAo group is higher than that in the 5-min tCCAo group. Scale bar=50 μ m. (I) ROD of Iba-1 immunoreactive structures. The bars indicate the means \pm SD ($n=7$ at each time after tCCAo, * $P<0.05$, significantly different from the sham group, † $P<0.05$, significantly different from the 5-min tCCAo group)

and 66.1% at 5 days) than that in the 5-min tCCAo group (Fig. 7Ae1, Af1 and C).

In the 5-min sham and 15-min sham groups, IL-1 β immunoreactivity was also found in pyramidal cells (Fig. 7Ba and Ba1), and the immunoreactivity in the two groups was similar to each other (Fig. 7Ba, Ba1 and D).

In the 5-min tCCAo group, IL-1 β immunoreactivity in the pyramidal cells was not altered at 6 h, decreased at 12 h (59.6%) and highest (172.3%) at 1 day after TI compared with that in the 5-min sham group (Fig. 7Bb, Bc, Bd and D). Thereafter IL-1 β immunoreactivity was decreased (158.1% at 2 days and 35.9% at 5 days compared with that in the 5-min sham group) (Fig. 7Be, Bf and D). In the 15-min tCCAo group, IL-1 β immunoreactivity in the pyramidal neurons was not also changed 6 h after tCCAo, increased until 1 day after tCCAo, showing that its ROD was 129.7% at 12 h and 238.3% at 1 day compared with that in the 5-min tCCAo group (Fig. 7Ba1, 7Bb1, 7Bc1 and 7D). Thereafter, IL-1 β immunoreactivity was also gradually decreased, but its ROD was also higher (126.5% at 2 day and 65.4% at 5 days) than that in the 5-min tCCAo group (Fig. 7Ae1, Af1 and C).

In this study, IL-4 and IL-13 immunohistochemistry was conducted to examine the changes of anti-inflammatory cytokines following tCCAo in the hippocampal CA1 region.

IL-4 immunoreactivity was weakly observed in pyramidal cells in both 5-min sham and 15-min sham groups (Fig. 8Aa and Aa1), showing that the immunoreactivity was not different between the two groups (Fig. 8C). In the 5-min tCCAo group, IL-4 immunoreactivity in the pyramidal cells was decreased with time after tCCAo, showing that, at 5 days after tCCAo, the IL-4 immunoreactivity was the lowest (37.5% of the 5-min sham group) (Fig. 8Aa–Af and C). In the 15-min tCCAo group, IL-4 immunoreactivity in the pyramidal neurons was also significantly decreased with time after tCCAo, showing that the immunoreactivity until 1 day after tCCAo was not significantly different from that in the 5-min tCCAo group but significantly lower at 2 days (25.9%) and 5 days (21.3%) after tCCAo than that in the 5-min tCCAo group (Fig. 8Aa1–Af1 and C).

Strong IL-13 immunoreactivity was shown in pyramidal neurons in both 5-min sham and 15-min sham groups (Fig. 8Ba and Ba1), and the immunoreactivity was similar to each other (Fig. 8D). In the 5-min tCCAo group, IL-13 immunoreactivity in the pyramidal cells was gradually from 6 h after tCCAo, and, at 5 days after tCCAo, the IL-13 immunoreactivity was the lowest (21.2% of the 5-min sham group) (Fig. 8Ba–Bf and D). In the 15-min tCCAo group, IL-13 immunoreactivity in the pyramidal neurons was also significantly decreased with time after tCCAo, but the immunoreactivity at all points in time after tCCAo was significantly lower than that in the 5-min tCCAo group, showing that the ROD was 70.8% at 6 h, 48.1% at 12 h, 34.9% at 1 day, 19.4% at 2 days and 14.5% at 5 days after tCCAo compared with that in the 5-min tCCAo group (Fig. 8Aa1–Af1 and D).

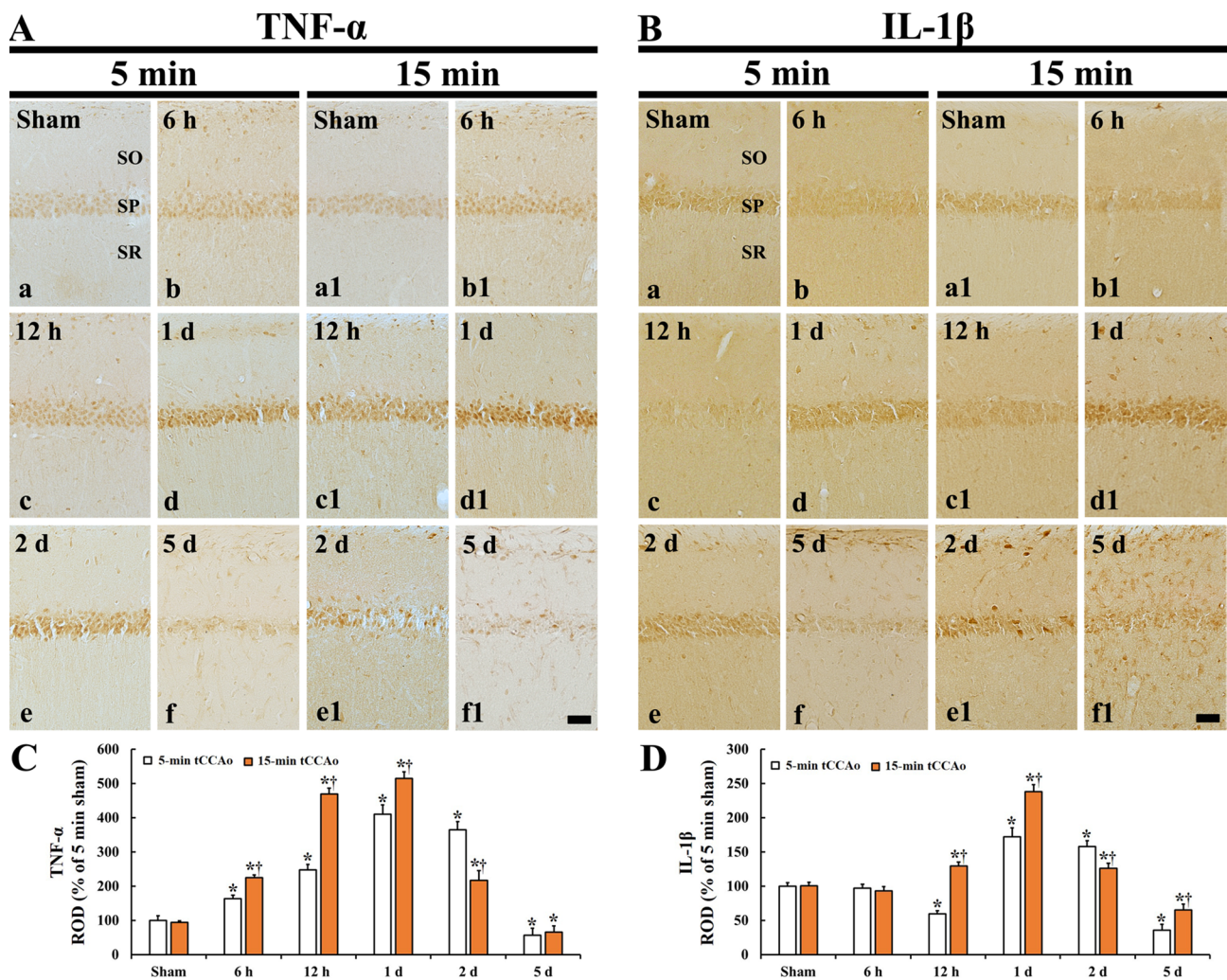


Fig. 7 Immunohistochemistry for TNF- α (A) and IL-1 β (B) in the CA1 region at sham (a, a1), 6 h (b, b1), 12 h (c, c1), 1 day (d, d1), 2 days (e, e1), and 5 days (f, f1) in the 5-min (a–f) and 15-min (a1–f1) tCCAo groups. TNF- α immunoreactivity is shown in pyramidal cells and gradually increased until 1 day after tCCAo. In the 15-min tCCAo group, TNF- α immunoreactivity is also gradually increased until 1 day after tCCAo, showing that the immunoreactivity is significantly higher than that in the 5-min tCCAo group. IL-1 β immunoreactivity is also found in pyramidal cells. IL-1 β immunoreactiv-

ity in the 5-min tCCAo group is significantly increased 1 day after tCCAo and then decreased. In the 15-min tCCAo group, IL-1 β immunoreactivity is altered like the change of TNF- α , showing that the immunoreactivity is significantly high compared with that in the 5-min tCCAo group. Scale bar=50 μ m. (C, D) ROD of TNF- α (C) and IL-1 β (D) immunoreactive structures in the SP. The bars indicate the means \pm SD (n=7 at each time after tCCAo TI, *P<0.05, significantly different from sham group, †P<0.05, significantly different from 5-min tCCAo group)

Discussion

In the present study, to investigate the possible mechanisms of neuronal death after tCCAo, we examined differences in neuronal damage, BBB permeability (leakage of albumin and IgG), microgliosis, and inflammatory cytokine expression in the gerbil hippocampal CA1 region, which is vulnerable to tCCAo, following 5-min and 15-min tCCAo using immunohistochemistry.

In the present study, we found that the neuronal damage and death induced by 15-min tCCAo occurred much earlier and was more severe than that induced by 15-min tCCAo

in pyramidal neurons, which are the principal neurons in the stratum pyramidale (SP) of the CA1 region. This finding confirmed the results of a previous study showing that neuronal damage/death in the CA1 region of the gerbil hippocampus occurred much more rapidly and was more severe after longer-duration ischemia [32]. In addition, more severe tissue injury was observed in the rat brain after middle cerebral artery occlusion (MCAO) with increased ischemic duration [43]. However, even brief ischemic episodes of at least 5-min cause neuronal death in the CA1 region that is irreversible from 5 days after tCCAo [44, 45], which results in a decrease in short-term memory function [46, 47].

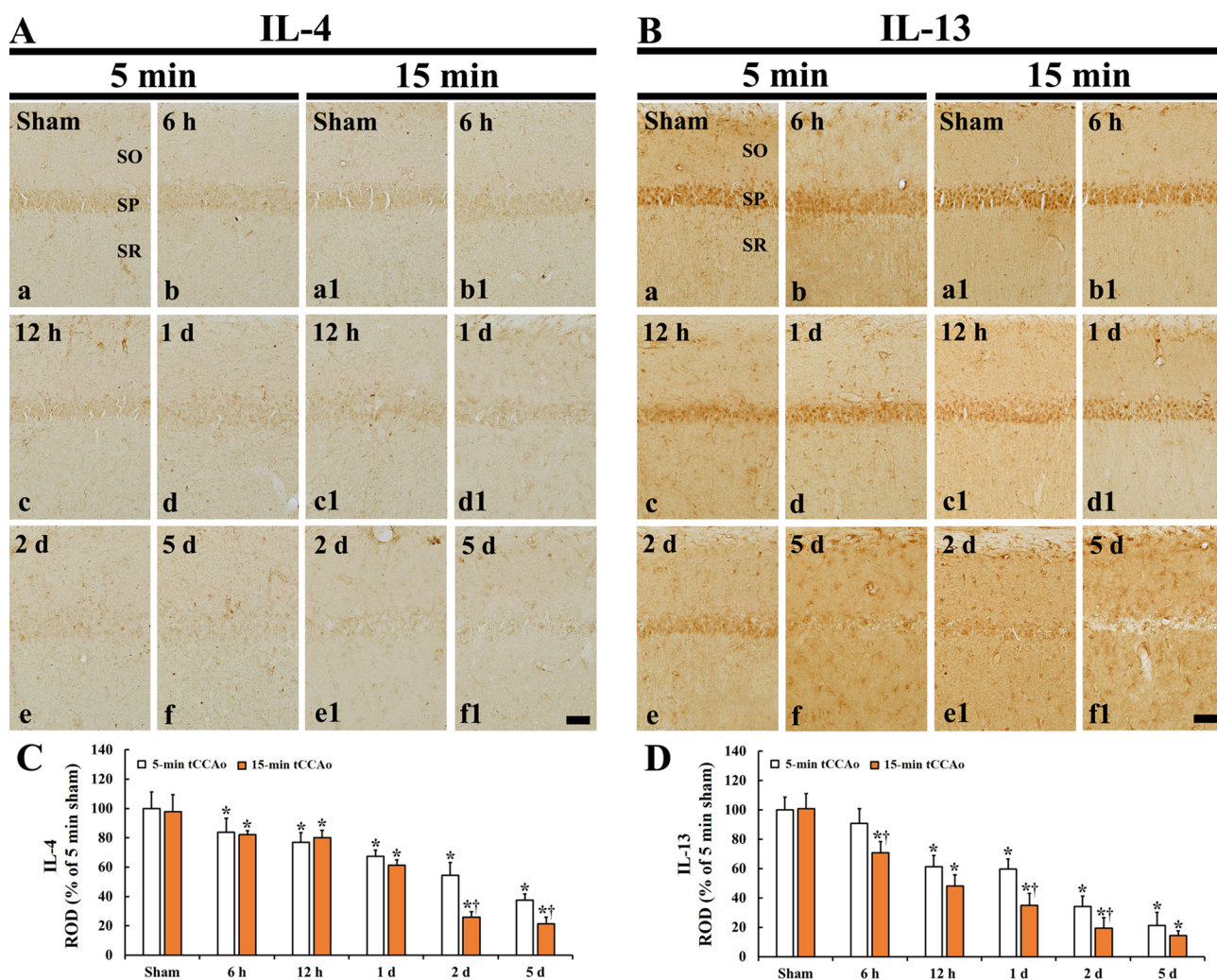


Fig. 8 **A, B** Immunohistochemistry for IL-4 (**A**) and IL-13 (**B**) in the CA1 region at sham (**a, a1**), 6 h (**b, b1**), 12 h (**c, c1**), 1 day (**d, d1**), 2 days (**e, e1**), and 5 days (**f, f1**) in the 5-min (**a–f**) and 15-min (**a1–f1**) tCCAo group. IL-4 immunoreactivity is shown in pyramidal neurons and gradually decreased after tCCAo. In the 15-min tCCAo group, IL-4 immunoreactivity until 1 day after tCCAo is similar to that in the 5-min tCCAo group, but significantly lower at 2 and 5 days than that in the 5-min tCCAo group. IL-3 immunoreactivity is also

found in pyramidal cells and gradually decreased after tCCAo. In the 15-min tCCAo group, IL-3 immunoreactivity is significantly low at all points in time compared with that in the 5-min tCCAo group. Scale bar = 50 μ m. (**C, D**) ROD of IL-4 (**C**) and IL-13 (**D**) immunoreactive structures in the SP. The bars indicate the means \pm SD ($n=7$ at each time after tCCAo, * $P<0.05$, significantly different from sham group, $^{\dagger}P<0.05$, significantly different from 5-min tCCAo group)

BBB leakage is known as one of the common pathological features in brain diseases involving ischemia. Assessment of leakage of serum albumin and IgG is widely used to determine BBB disruption following cerebral ischemia [18, 27–29, 48]. A prior study reported that extravasation of serum proteins, such as IgG, albumin and complement factor C3, was detected in ipsilateral ischemic tissues and sometimes in ischemic tissues of the contralateral hemisphere following focal ischemia induced by MCAO in rats [49]. Also, the degree of it was reported that BBB permeability, assessed by IgG extravasation, was significantly increased in the ipsilateral cerebral cortex following MCAO in rats [25]. In the current study, we found that significant leakage of

albumin and IgG in the CA1 region began at 1 or 2 days after 5-min tCCAo and that albumin and IgG immunoreactivity was markedly increased at 5 days after 5-min tCCAo. This finding is consistent with that of studies showing that serum albumin [42] and IgG [37] extravasation occurred in the gerbil CA1 region at 2 days after 5-min tCCAo and albumin and IgG immunoreactivity was significantly increased at 5 days post-tCCAo. Additionally, we found that albumin and IgG leakage was more severe and occurred at earlier time points following 15-min tCCAo vs. 5-min tCCAo and the immunoreactivities of albumin and IgG in the 15-min tCCAo group was significantly greater at all post-tCCAo time points than that in the 5-min tCCAo group. This result indicates that

more severe BBB leakage occurs more quickly in the CA1 region following 15-min tCCAO compared to 5-min tCCAO; it is in line with the results of a previous study showing that increased duration of tCCAO causes more severe vascular disruption and IgG leakage in the rat brain following MCAO and implies that more severe BBB disruption is closely related to an increase in ischemic duration [43]. To the best of our knowledge, this is the first study confirm the changes in BBB permeability with different duration of ischemia in a gerbil model of transient cerebral ischemia, not focal ischemia leading necrosis.

We recently reported that albumin immunoreactivity was markedly increased in Iba-1-immunoreactive microglia and pyramidal neurons in the gerbil hippocampal CA1 region after 5-min tCCAO [42]. In the current study, we also found that IgG immunoreactivity was observed in NeuN-immunoreactive neurons and Iba-1-immunoreactive microglia in the CA1 region following 5-min and 15-min tCCAO, showing that, in particular, weak IgG immunoreactivity began appear in microglia at 1 day after 5-min tCCAO and at 6 h after 15-min tCCAO, and that the extent of IgG immunoreactivity in the 15-min tCCAO group was significantly stronger than that in the 5-min tCCAO group. Michalski et al. reported that IgG and FITC-albumin immunoreactivity was observed in neurons and activated microglia in rat brain tissue following MCAO [28]. In addition, Zhang et al. reported that IgG immunoreactivity was shown in neuronal cell bodies and rat brain parenchyma at 14 days after MCAO [26]. Furthermore, Michalak et al. reported that IgG accumulated in human and rodent hippocampal neurons following epileptic episodes, and they suggested that IgG leakage might lead to neuronal dysfunction and degeneration [50]. Taken together, these results imply that extravasated albumin and IgG is ingested or bounded by activated microglia and neurons and that, especially, IgG accumulation in neurons can contribute to tCCAO-induced delayed neuronal death.

It has been theorized that BBB damage and extravasation of serum proteins can promote activation of the immune response, which contributes to cell death in injured brain regions after ischemia [49]. Microglia that are activated before neuronal death participate in various responses, including microglia-mediated cytokine release (such as TNF- α , IL-1 β , interferon- γ , etc.), which enhances the inflammatory process, contributes to BBB damage, and results in ischemic neuronal death [51, 52]. Activation of microglia with morphological changes and increased immunoreactivity in response to ischemic injury has been reported in the CA1 region after tCCAO in gerbils [53, 54]. In our current study, Iba-1 immunoreactive microglia were activated after both 5-min and 15-min tCCAO. However, the activated microglia became aggregated in the SP earlier in the 15-min tCCAO group than in the 5-min tCCAO

group. Half of all pyramidal cells located in the SP were lost after 15-min tCCAO. While the same cells remained alive in the 5-min tCCAO group. This finding is in agreement with some studies showing excessive microglia activation and clustering at the site of accelerated neuronal death in the hippocampal CA1 region after longer-duration tCCAO in rodents, suggesting that the observed microglia must be blood-derived phagocytic macrophages [41, 55].

It has been reported that albumin can access central nervous system (CNS) tissue following BBB damage and leakage and that this albumin can be exposed to inflammatory processes and tissue damage [17]. In addition, IgG in brain parenchyma can trigger a detrimental inflammatory response by producing TNF- α through the formation of immune complexes with microglia in responses to brain diseases [56]. Yang et al. recently reported that an intracerebral injection of IgG from lupus serum induced microglial activation and increased expression of pro-inflammatory cytokines (IL-1 β , TNF- α and IL-6) in brain tissue [57]. In addition, Clausen et al. reported that TNF- α and IL-1 β were expressed in neurons and microglia in ischemic brain [58]. Similar to these previous findings, in the current research, 15-min tCCAO significantly increased pro-inflammatory cytokine (TNF- α and IL-1 β) immunoreactivity in the ischemic CA1 region and significantly reduced the immunoreactivities of anti-inflammatory cytokines (IL-4 and IL-13) compared with those in the 5-min tCCAO group. This finding corresponded with the significantly increased immunoreactivities of albumin and IgG, and microglial activation in the 15-min tCCAO group. In a recent study by Ronaldson et al., when resting microglia were activated under pathological stress and polarized to M1 microglia, expression of pro-inflammatory cytokines (TNF- α , IL-1 β , IL-6, and IL-12 etc.) increased leading to BBB dysfunction, whereas, when the microglia polarized to M2 microglia, anti-inflammatory cytokine (IL-10, transforming growth factor- β 1) expression increased, which helped protect the BBB [59]. Together, all of these results indicate that an increase in pro-inflammatory cytokine expression and a decrease in anti-inflammatory cytokine expression after tCCAO are closely related to leakage of serum proteins and activation of microglia and that the degree of cytokine expression is dependent on tCCAO duration.

In conclusion, the current study showed that 15-min tCCAO accelerated neuronal damage in gerbil hippocampal CA1 region due to earlier and more severe increases in BBB permeability (albumin and IgG leakage), microglial activation and pro-inflammatory cytokine production than 5-min tCCAO. Based on these results, in-depth research on inhibition of neuronal death via regulation of BBB permeability should be conducted in the future. Based on these results, in-depth research on inhibition of neuronal death via regulation of BBB permeability should be conducted in the future.

Author Contributions The author's individual contributions is provided as follow; "Conceptualization, CL, JA, MW and SC; methodology, TL, BK, and HS; software, TL, BK, and HS; validation, CL, JA, MW, SC, JL, MS, JC, and DK; formal analysis, TL, BK, HS, JL, MS, JC, and DK; investigation, TL, BK, HS, JL, MS, JC, and DK; resources, MW and SC; data cu-ration, CL and JA; writing—original draft preparation, CL and JA; writing—review and editing, MW and SC; visualization, JA, CL; supervision, MW and SC; project administration, CL, JA, MW and SC; funding acquisition, MW and SC. All authors have read and agreed to the published version of the manuscript.

Funding This research was funded by Basic Science Research Program through the National Research Foundation of Korea (NRF) funded by the Ministry of Education, grant number NRF-2020R1F1A1052380 and NRF-2019R1A6A1A11036849".

Data Availability All data generated or analyzed during this study are included in this published article.

Declarations

Conflict of interest The authors have declared that there are no competing interests.

Ethical Approval The process of handling and caring animals conformed to the guidelines from the current international laws and policies in the "NIH Guide for the Care and Use of Laboratory Animals" (The National Academies Press, 8th Ed., 2011). The protocol of this experiment was approved (approval no. KW-2000113-1) by the Institutional Animal Care and Use Committee (IACUC) at Kangwon National University.

References

- Araki T, Kato H, Kogure K (1989) Selective neuronal vulnerability following transient cerebral ischemia in the gerbil: distribution and time course. *Acta Neurol Scand* 80:548–553
- Candelario-Jalil E, Mhadu NH, Al-Dalain SM et al (2001) Time course of oxidative damage in different brain regions following transient cerebral ischemia in gerbils. *Neurosci Res* 41:233–241
- Kirino T (1982) Delayed neuronal death in the gerbil hippocampus following ischemia. *Brain Res* 239:57–69
- Kirino T, Sano K (1984) Selective vulnerability in the gerbil hippocampus following transient ischemia. *Acta Neuropathol* 62:201–208
- Medvedeva YV, Ji SG, Yin HZ et al (2017) Differential vulnerability of CA1 versus CA3 pyramidal neurons after ischemia: possible relationship to sources of Zn²⁺ accumulation and its entry into and prolonged effects on mitochondria. *J Neurosci* 37:726–737
- Zhang M, Li W-B, Liu Y-X et al (2011) High expression of GLT-1 in hippocampal CA3 and dentate gyrus subfields contributes to their inherent resistance to ischemia in rats. *Neurochem Int* 59:1019–1028
- Zou B, Li Y, Deng P et al (2005) Alterations of potassium currents in ischemia-vulnerable and ischemia-resistant neurons in the hippocampus after ischemia. *Brain Res* 1033:78–89
- Kirino T, Sano K (1984) Fine structural nature of delayed neuronal death following ischemia in the gerbil hippocampus. *Acta Neuropathol* 62:209–218
- Johansen FF, Jørgensen MB, Diemer N (1983) Resistance of hippocampal CA-1 interneurons to 20 min of transient cerebral ischemia in the rat. *Acta Neuropathol* 61:135–140
- Nitsch C, Scotti A, Sommacal A et al (1989) GABAergic hippocampal neurons resistant to ischemia-induced neuronal death contain the Ca²⁺-binding protein parvalbumin. *Neurosci Lett* 105:263–268
- Doyle KP, Simon RP, Stenzel-Poore MP (2008) Mechanisms of ischemic brain damage. *Neuropharmacology* 55:310–318
- Harukuni I, Bhardwaj A (2006) Mechanisms of brain injury after global cerebral ischemia. *Neurol Clin* 24:1–21
- Lee J-C, Park CW, Shin MC et al (2018) Tumor necrosis factor receptor 2 is required for ischemic preconditioning-mediated neuroprotection in the hippocampus following a subsequent longer transient cerebral ischemia. *Neurochem Int* 118:292–303
- Park CW, Ahn JH, Lee T-K et al (2020) Post-treatment with oxcarbazepine confers potent neuroprotection against transient global cerebral ischemic injury by activating Nrf2 defense pathway. *Biomed Pharmacother* 124:109850
- Neuwelt EA, Bauer B, Fahlke C et al (2011) Engaging neuroscience to advance translational research in brain barrier biology. *Nat Rev Neurosci* 12:169–182
- Liu Z, Liu J, Wang S et al (2016) Neuronal uptake of serum albumin is associated with neuron damage during the development of epilepsy. *Exp Ther Med* 12:695–701
- LeVine SM (2016) Albumin and multiple sclerosis. *BMC Neurol* 16:1–12
- Kassner A, Merali Z (2015) Assessment of blood-brain barrier disruption in stroke. *Stroke* 46:3310–3315
- Tang XN, Cairns B, Kim JY et al (2012) NADPH oxidase in stroke and cerebrovascular disease. *Neurol Res* 34:338–345
- Wang Q, Tang XN, Yenari MA (2007) The inflammatory response in stroke. *J Neuroimmunol* 184:53–68
- Chung TN, Kim JH, Choi BY et al (2015) Adipose-derived mesenchymal stem cells reduce neuronal death after transient global cerebral ischemia through prevention of blood-brain barrier disruption and endothelial damage. *Stem Cells Transl Med* 4:178–185
- Lan XB, Wang Q, Yang JM et al (2019) Neuroprotective effect of Vanillin on hypoxic-ischemic brain damage in neonatal rats. *Biomed Pharmacother* 118:109196
- Preston E, Webster J (2004) A two-hour window for hypothermic modulation of early events that impact delayed opening of the rat blood-brain barrier after ischemia. *Acta Neuropathol* 108:406–412
- Woodruff TM, Thundiyil J, Tang SC et al (2011) Pathophysiology, treatment, and animal and cellular models of human ischemic stroke. *Mol Neurodegener* 6:11
- Yang C, DeMars KM, Alexander JC et al (2017) Sustained neurological recovery after stroke in aged rats treated with a novel prostacyclin analog. *Stroke* 48:1948–1956
- Zhang X, Chen XP, Lin JB et al (2017) Effect of enriched environment on angiogenesis and neurological functions in rats with focal cerebral ischemia. *Brain Res* 1655:176–185
- Maeda M, Akai F, Nishida S et al (1992) Intracerebral distribution of albumin after transient cerebral ischemia: light and electron microscopic immunocytochemical investigation. *Acta Neuropathol* 84:59–66
- Michalski D, Grosche J, Pelz J et al (2010) A novel quantification of blood-brain barrier damage and histochemical typing after embolic stroke in rats. *Brain Res* 1359:186–200
- Ye XL, Lu LQ, Li W et al (2017) Oral administration of ampelopsin protects against acute brain injury in rats following focal cerebral ischemia. *Exp Ther Med* 13:1725–1734
- Borlongan CV, Yamamoto M, Takei N et al (2000) Glial cell survival is enhanced during melatonin-induced neuroprotection against cerebral ischemia. *FASEB J* 14:1307–1317
- Nordborg C, Sokrab T, Johansson B (1991) The relationship between plasma protein extravasation and remote tissue changes after experimental brain infarction. *Acta Neuropathol* 82:118–126

32. Lee TK, Kim H, Song M et al (2019) Time-course pattern of neuronal loss and gliosis in gerbil hippocampi following mild, severe, or lethal transient global cerebral ischemia. *Neural Regen Res* 14:1394–1403
33. Yu DK, Yoo KY, Shin BN et al (2012) Neuronal damage in hippocampal subregions induced by various durations of transient cerebral ischemia in gerbils using Fluoro-Jade B histofluorescence. *Brain Res* 1437:50–57
34. Lee J-C, Ahn JH, Lee DH et al (2013) Neuronal damage and gliosis in the somatosensory cortex induced by various durations of transient cerebral ischemia in gerbils. *Brain Res* 1510:78–88
35. Ohk TG, Yoo K-Y, Park SM et al (2012) Neuronal damage using fluoro-jade B histofluorescence and gliosis in the striatum after various durations of transient cerebral ischemia in gerbils. *Neurochem Res* 37:826–834
36. Park CW, Lee J-C, Ahn JH et al (2013) Neuronal damage using fluoro-Jade B histofluorescence and gliosis in the gerbil septum submitted to various durations of cerebral ischemia. *Cell Mol Neurobiol* 33:991–1001
37. Ahn JH, Chen BH, Park JH et al (2018) Early IV-injected human dermis-derived mesenchymal stem cells after transient global cerebral ischemia do not pass through damaged blood–brain barrier. *J Tissue Eng Regen Med* 12:1646–1657
38. Park JH, Kim DW, Lee TK et al (2019) Improved HCN channels in pyramidal neurons and their new expression levels in pericytes and astrocytes in the gerbil hippocampal CA1 subfield following transient ischemia. *Int J Mol Med* 44:1801–1810
39. Radtke-Schuller S, Schuller G, Angenstein F et al (2016) Brain atlas of the Mongolian gerbil (*Meriones unguiculatus*) in CT/MRI-aided stereotaxic coordinates. *Brain Struct Funct* 221:1–272
40. Schmued LC, Hopkins KJ (2000) Fluoro-Jade B: a high affinity fluorescent marker for the localization of neuronal degeneration. *Brain Res* 874:123–130
41. Sugawara T, Lewén A, Noshita N et al (2002) Effects of global ischemia duration on neuronal, astroglial, oligodendroglial, and microglial reactions in the vulnerable hippocampal CA1 subregion in rats. *J Neurotrauma* 19:85–98
42. Park JH, Park JA, Ahn JH et al (2017) Transient cerebral ischemia induces albumin expression in microglia only in the CA1 region of the gerbil hippocampus. *Mol Med Rep* 16:661–665
43. Chen B, Friedman B, Cheng Q et al (2009) Severe blood–brain barrier disruption and surrounding tissue injury. *Stroke* 40:e666–674
44. Kim H, Park JH, Shin MC et al (2019) Fate of astrocytes in the gerbil hippocampus after transient global cerebral ischemia. *Int J Mol Sci* 20:845
45. Lee CH, Moon SM, Yoo K-Y et al (2010) Long-term changes in neuronal degeneration and microglial activation in the hippocampal CA1 region after experimental transient cerebral ischemic damage. *Brain Res* 1342:138–149
46. Ahn JH, Choi JH, Park JH et al (2016) Long-term exercise improves memory deficits via restoration of myelin and microvessel damage, and enhancement of neurogenesis in the aged gerbil hippocampus after ischemic stroke. *Neurorehabil Neural Repair* 30:894–905
47. Lee JC, Park JH, Ahn JH et al (2016) New GABAergic neurogenesis in the hippocampal CA1 region of a gerbil model of long-term survival after transient cerebral ischemic injury. *Brain Pathol* 26:581–592
48. Jørgensen MB, Finsen BR, Jensen MB et al (1993) Microglial and astroglial reactions to ischemic and kainic acid-induced lesions of the adult rat hippocampus. *Exp Neurol* 120:70–88
49. Nishino H, Czurko A, Fukuda A et al (1994) Pathophysiological process after transient ischemia of the middle cerebral artery in the rat. *Brain Res Bull* 35:51–56
50. Michalak Z, Lebrun A, Di Miceli M et al (2012) IgG leakage may contribute to neuronal dysfunction in drug-refractory epilepsies with blood–brain barrier disruption. *J Neuropathol Exp Neurol* 71:826–838
51. da Fonseca ACC, Matias D, Garcia C et al (2014) The impact of microglial activation on blood–brain barrier in brain diseases. *Front Cell Neurosci* 8:362
52. Yenari MA, Xu L, Tang XN et al (2006) Microglia potentiate damage to blood–brain barrier constituents: improvement by minocycline in vivo and in vitro. *Stroke* 37:1087–1093
53. Hwang IK, Park JH, Lee TK et al (2017) CD74-immunoreactive activated M1 microglia are shown late in the gerbil hippocampal CA1 region following transient cerebral ischemia. *Mol Med Rep* 15:4148–4154
54. Hwang IK, Yoo K-Y, Kim DW et al (2006) Ionized calcium-binding adapter molecule 1 immunoreactive cells change in the gerbil hippocampal CA1 region after ischemia/reperfusion. *Neurochem Res* 31:957–965
55. Yan BC, Ohk TG, Ahn JH et al (2014) Differences in neuronal damage and gliosis in the hippocampus between young and adult gerbils induced by long duration of transient cerebral ischemia. *J Neurol Sci* 337:129–136
56. Hulse RE, Swenson WG, Kunkler PE et al (2008) Monomeric IgG is neuroprotective via enhancing microglial recycling endocytosis and TNF- α . *J Neurosci* 28:12199–12211
57. Yang C, Hou X, Feng Q et al (2019) Lupus serum IgG induces microglia activation through Fc fragment dependent way and modulated by B-cell activating factor. *J Transl Med* 17:1–15
58. Clausen BH, Wirenfeldt M, Høgedal SS et al (2020) Characterization of the TNF and IL-1 systems in human brain and blood after ischemic stroke. *Acta Neuropathol Commun* 8:1–17
59. Ronaldson PT, Davis TP (2020) Regulation of blood–brain barrier integrity by microglia in health and disease: a therapeutic opportunity. *J Cereb Blood Flow Metab* 40:S6–S24

Publisher's Note Springer Nature remains neutral with regard to jurisdictional claims in published maps and institutional affiliations.

Authors and Affiliations

Choong-Hyun Lee¹ · Ji Hyeon Ahn^{2,3} · Tae-Kyeong Lee⁴ · Hyejin Sim³ · Jae-Chul Lee³ · Joon Ha Park⁵ · Myoung Cheol Shin⁶ · Jun Hwi Cho⁶ · Dae Won Kim⁷ · Moo-Ho Won³  · Soo Young Choi⁴

¹ Department of Pharmacy, College of Pharmacy, Dankook University, Cheonan, Chungnam 31116, Republic of Korea

² Department of Physical Therapy, College of Health Science, Youngsan University, Yangsan, Gyeongnam 50510, Republic of Korea

- ³ Department of Neurobiology, School of Medicine, Kangwon National University, Chuncheon, Gangwon 24341, Republic of Korea
- ⁴ Department of Biomedical Science, Research Institute of Bioscience and Biotechnology, Hallym University, Chuncheon, Gangwon 24252, Republic of Korea
- ⁵ Department of Anatomy, College of Korean Medicine, Dongguk University, Gyeongju, Gyeongbuk 38066, Republic of Korea
- ⁶ Department of Emergency Medicine, School of Medicine, Kangwon National University Hospital, Kangwon National University, Chuncheon, Gangwon 24289, Republic of Korea
- ⁷ Department of Biochemistry and Molecular Biology, and Research Institute of Oral Sciences, College of Dentistry, Gangnung-Wonju National University, Gangneung, Gangwon 25457, Republic of Korea